International Journal of Pharmaceutics 486 (2015) 339–349

Contents lists available at ScienceDirect

International Journal of Pharmaceutics

journal homepage: www.elsevier.com/locate/ijpharm

A miniaturized *in vitro* release method for investigating drug-release mechanisms

E. Ahnfelt, E. Sjögren, N. Axén, H. Lennernäs *

Department of Pharmacy, Uppsala University, Box 580, 751 23 Uppsala, Sweden

ARTICLE INFO

Article history:
Received 26 February 2015
Received in revised form 30 March 2015
Accepted 31 March 2015
Available online 2 April 2015

Keywords:
In vitro release methods
Release mechanisms
Weibull function
GI-Sim
In vivo prediction

ABSTRACT

We have evaluated a miniaturized *in vitro* method, based on the μDISS Profiler™ technique that enables on-line monitoring of drug release from a 21 μl sample with 10 ml of release medium. Four model drugs in eight clinically used formulations, including both solid and non-solid drug delivery systems, were investigated. The acquired data were compared with historical *in vitro* release data from the same formulations. Use of the Weibull function to describe the *in vitro* drug-release profiles allowed discrimination between the selected formulations with respect to the drug-release mechanisms. Comparison of the release data from the same formulation in different *in vitro* set-ups showed that the methodology used can affect the mechanism of *in vitro* release. We also evaluated the ability of the *in vitro* methods to predict *in vivo* activity by comparing simulated plasma concentration-time profiles acquired from the application of the biopharmaceutical software GI-Sim to the *in vitro* observations. In summary, the simulations based on the miniaturized-method release data predicted the plasma profiles as well as or more accurately than simulations based on the historical release data in 71% of the cases and this miniaturized *in vitro* method appears to be applicable for both solid and non-solid formulations.

1. Introduction

Successful drug development processes benefit from the combination of *in vitro* methods and *in silico* simulations that can predict the *in vivo* response (Lennernäs et al., 2014a). To enable accurate *in vivo* predictions from *in vitro* drug-release data, the drug must be released from the formulation by a similar mechanism both *in vivo* and *in vitro* (Larsen et al., 2013). There are standardized *in vitro* quality control release methods for oral formulations, as described for example in the US Pharmacopeia (USP). The USP experimental set-ups include the paddle, rotation and reciprocating cylinder apparatuses. However, these methods might not always be accurately predictive of the *in vivo* situation (Kostewicz et al., 2014b). Adjustments to the stirring rate, temperature and release medium (surfactant, ionic strength and pH) could alter the release rates to varying degrees, and information on this would be of value for accelerated and biorelevant *in vitro* release studies of modified-release formulations (Shen and Burgess, 2012). The use of a biorelevant medium that mimics the dynamic gastrointestinal fluid has also been shown to increase the predictability of *in vitro* methods (Klein, 2010; Kostewicz et al., 2014b).

The μDISS profiler™, a miniaturized dissolution apparatus that uses only small amounts of active pharmaceutical ingredient (API) and release medium, was developed to measure the solubility of APIs in early drug development (Fagerberg et al., 2010; Tsinman et al., 2009). Importantly, this apparatus continuously monitors absorbance, using a fiber-optic UV dip probe located centrally in a glass vial (Avdeef and Tsinman, 2008). The mini-IDR™ disc, an additional application for the μDISS profiler™, enables measurement of the intrinsic dissolution rate (IDR). Because the exposed area of the API is constant when measuring the IDR, it has been used to characterize dissolution profiles (Avdeef and Tsinman, 2008).

Theoretical modeling is a useful tool in pharmaceutical development; it is used to investigate and characterize the release of the API from the drug delivery system (DDS) and to determine which factors influence the release rate (Siepmann and Siepmann, 2012). This type of knowledge is also useful during the innovation

* Corresponding author. Tel.: +46 18 471 4317; fax: +46 18 471 4223.
E-mail address: hans.lennernas@farmaci.uu.se (H. Lennernäs).

http://dx.doi.org/10.1016/j.ijpharm.2015.03.076
0378-5173/

and development of novel DDSs where a specifically designed drug-release profile is needed to target specific pharmacodynamic and safety properties (Johannsson et al., 2011; Selen et al., 2014; Siepmann and Siepmann, 2012; Sjögren et al., 2014).

The primary objective of this study was to improve understanding of the novel, miniaturized, *in vitro*, μDISS™-based release method and to examine its potential for predicting *in vivo* data. The *in vivo* predictive abilities of release data from this novel method and of historical *in vitro* release data were compared using *in silico* simulations and the mechanisms of API release from selected DDSs were investigated using the Weibull function.

2. Materials and methods

2.1. Chemicals and drug delivery systems

Four APIs (metoprolol, diclofenac, naproxen and carbamazepine (Sigma–Aldrich, Sweden)), representing biopharmaceutics classification system (BCS) classes I and II (Wu and Benet, 2005), were investigated. Their physicochemical properties are listed in Table 1. The chosen drugs have typical physicochemical properties for drugs that are formulated in modified release dosage forms. The lipophilicity (log P) covers a three-fold range but the molecular weight covered a narrow range. Stock solutions were prepared by dissolving each API in ethanol (Solveco, Sweden). Mono- and dibasic potassium phosphate, used to prepare phosphate buffer saline (PBS), was acquired from Riedel de Haën, Germany.

The *in vitro* release profiles of eight clinically used DDSs were investigated. Two of the DDSs were non-solid formulations (an oral suspension and a gel for dermal application), two were oral modified-release (MR) tablets, and four were oral immediate-release (IR) tablets. The IR tablets contained metoprolol tartrate (Seloken™ 50 mg, Astra Zeneca, Sweden), naproxen (Pronaxen™ 250 mg, Orion Pharma, Sweden), carbamazepine (Tegretol™ 100 mg, Novartis, Sweden), and diclofenac (Voltaren T™ 25 mg, Novartis, Sweden). The MR tablets contained metoprolol succinate (Seloken ZOC™ 25 mg, Astra Zeneca, Sweden), and carbamazepine (Tegretol Retard™ 200 mg, Novartis, Sweden). The non-solid DDSs were a diclofenac dermal gel (Voltaren™ gel 11.6 mg/g), and an oral suspension of carbamazepine (Tegretol™ oral suspension 20 mg/ml), both from Novartis, Sweden.

2.2. Sample reservoirs for the modified μDISS™-based release method

The dimensions of the mini-IDR™ disc were used as a starting point for developing a sample reservoir made of magnetic ferritic stainless steel, an Fe–Cr alloy (Olsson and Landolt, 2003). A small cylindrical cavity, 3 mm deep and 3 mm in diameter, with a sample volume of 21 μl, was drilled centrally in the steel disc (Fig. 1). The opening was covered with a diffusion barrier (see description below) to retain the formulation sample in the reservoir. The diffusion barrier was held in place with a ring-shaped magnet placed centrally over the reservoir opening (Fig. 1).

Table 1
Physicochemical properties of the active pharmaceutical ingredients (APIs) included in the study.

API	Mw	S_0	pK_a	log P	BCS class
Metoprolol	267.37[a]	200[f]700[g,e]	9.7 (base)[b]	1.88[a]	I
Diclofenac	296.16[a]	0.375[a]	3.8 (acid)[c]	4.51[a]	II
Naproxen	230.27[a]	0.115[a]	4.4 (acid)[b]	3.18[a]	II
Carbamazepine	236.28[a]	0.256[a]	14 (base)[d]	2.45[a]	II

BCS: biopharmaceutical classification system; log P: logarithm of the partitioning coefficient; Mw: molecular weight; pK_a: acid dissociation constant; S_0: solubility (mg/ml).
[a] Benet et al. (2011).
[b] Fagerholm et al. (1997).
[c] O'Connor and Corrigan (2001).
[d] Scheytt et al. (2005).
[e] Ragnarsson et al. (1987).
[f] Metoprolol succinate.
[g] Metoprolol tartrate.

2.3. Experimental design

A μDiss profiler™ (p*ION*, USA) was used for all of the miniaturized *in vitro* release experiments (Fig. 1). The UV dip probe in the μDiss profiler™ automatically performs spectral scans at intervals of 200–720 nm and calculates the drug concentration as the area under the concentration-time curve (AUC) of the second derivate spectrum. The second derivate spectrum enhances the peaks and reduces baseline shifting of the UV spectrum, which reduces the effects of background turbidity (Avdeef et al., 2009; Bijlani et al., 2007). The drug release studies were performed in triplicate; for each experiment, a 21 μl sample was inserted into the sample reservoir and 10 ml of PBS buffer, pH 7.4, was added. A pH of 7.4 was chosen mainly because the method is intended for use with drugs delivered parenterally. However, it should be noted that the average ionization of the APIs at this pH was no different from that at the intestinal pH of 6.8. If not otherwise stated, the stirring rate was set at 400 rpm. A nylon mesh filter (pore size 150 μm), a polyvinylidene fluoride filter (pore size 0.45 μm) and a cellulose-based dialysis membrane (approximate pore size 0.003 μm) were used as drug diffusion barriers. These diffusion barriers were soaked in de-ionized water for 10 min at room temperature before use. During the drug release experiments, the temperature was kept at 37 °C using a water bath (Lauda, Germany).

2.4. In vitro release studies

In the miniaturized method, *in vitro* studies investigated the effect of the choice of diffusion barrier on the time taken for metoprolol and diclofenac (dissolved in de-ionized water) to reach equilibrium, and the effect of the stirring rate (100–400 rpm) on the mass transport of metoprolol and diclofenac across the diffusion barrier. The polyvinylidene fluoride filter (pore size 0.45 μm) provided appropriate mass transport values for these APIs and was use as the diffusion barrier in the stirring-rate hydrodynamic experiments.

All the solid formulations except metoprolol MR were crushed and sieved (Retsch, Germany) to prepare the material for the

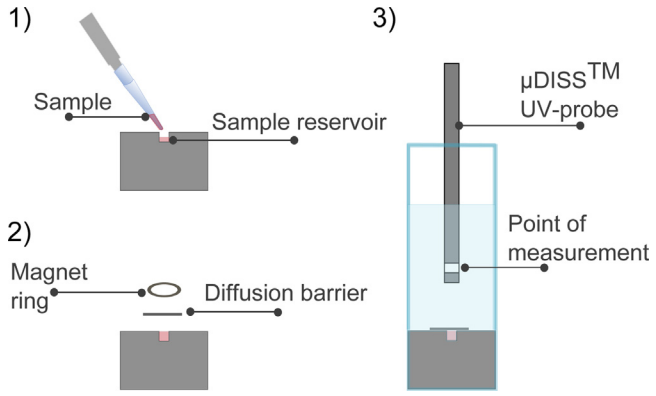

Fig. 1. A schematic illustration of the principles of the novel miniaturized *in vitro* release method. (1) The formulation sample is inserted into the sample reservoir. (2) The diffusion barrier is mounted and the ring-shaped magnet is attached to keep the diffusion barrier and the formulation sample in place. (3) The sample reservoir is placed in the glass vial and the release medium is added. The drug release is measured continuously with the μDISS™ UV-dip probe.

sample reservoir. The fraction of particles sized between 0.7 and 1.0 mm was collected and used for the *in vitro* release experiments. The matrix of the metoprolol MR tablet was dissolved in de-ionized water immediately prior to the experiment; within 5 min it disintegrated into small ethylcellulose-coated pellets (approximate size 0.5 mm) (Ragnarsson et al., 1987). Just before the start of the experiment, either the crushed particle fraction or the coated pellets were mixed with de-ionized water to create a slurry. 21 μl of the resulting slurry was inserted into the sample reservoir and covered with the diffusion barrier, in this case the nylon mesh filter (pore size 150 μm). The slurry was used to avoid air being trapped in the sample cavity and beneath the diffusion barrier, which could have reduced the mass transport of the API across the diffusion barrier. The non-solid DDSs (the gel and oral suspension) were inserted directly into the sample reservoir. All experiments were performed in triplicate.

Historical *in vitro* and *in vivo* data on the eight DDSs were collected from published reports (Al Ameri et al., 2012; Elqidra et al., 2004; Friedman et al., 2000; Gohel et al., 2009; Kovacevic et al., 2008; Löbenberg et al., 2005; Nan et al., 2012; Nishihata, 1987; Parsaee et al., 2002; Reiner et al., 2001; Sandberg et al., 1988; Yuksel et al., 2000; Zhang et al., 2011; Zhou et al., 1998) and obtained quantitatively with PlotDigitizer (Free Software Foundation Inc., MA, USA).

2.5. Data analysis

The nonlinear semi-log line of the software GraphPad Prism 6.04 (GraphPad Software, Inc., USA) was used to analyze the correlations between the pore size of the diffusion barrier and the time to equilibrium.

Many models are available for theoretically modeling drug-release mechanisms (Siepmann and Siepmann, 2008). However, the entire *in vitro* drug-release profile can be described by the Weibull function. In Eq. (1), the Weibull function has been slightly modified

$$R\%_t = R\%_{max} \times (1 - \exp^{-at^b}) \quad (1)$$

$R\%_t$ and $R\%_{max}$ are the percentage of drug released at time t and the maximum percentage released, respectively; a and b are constants describing the drug-release profile, and t is the time (Papadopoulou et al., 2006). The Weibull function has been reported to be useful in comparing release profiles for the delivery of drugs from various matrices (Dash et al., 2010). The combination of Monte Carlo simulations and experimental release data has shown that the values of b in the Weibull function can provide an indication of the release mechanisms involved in the drug release (Papadopoulou et al., 2006).

In this study, Eq. (1) was fitted to the observed data using the average value of each time point for both the experimental and the historical data. The curve fitting was performed using the nonlinear least square regression in Phoenix 64 WinNonlin 6.3 software (Pharsight, USA). Estimated a and b values were then used to extrapolate the release profiles for complete drug release. The goodness of fit for each analysis was expressed as the absolute average fold error (AAFE), as described by Graham et al. (2012).

$$\text{Absoluteaveragefolderror} = 10^{\frac{\sum|\log\frac{\text{Predicted}}{\text{Observed}}|}{N}} \quad (2)$$

AAFE describes the geometric mean ratio of the predicted and observed values and N describes the number of observations. An AAFE value of 1 indicates a perfect fit while a value of 2 indicates an average 2-fold difference from observed data points.

2.6. In silico simulations of in vivo response

In silico simulations based on the experimental and historical *in vitro* data were obtained using the gastrointestinal (GI) absorption model GI-Sim (Sjögren et al., 2013). Briefly, the GI-Sim simulates human GI physiology with nine simulated GI compartments. The GI compartments are connected in series to represent the stomach (compartment 1), the small intestine (compartments 2–7) and the colon (compartments 8–9) (Yu and Amidon, 1999; Yu et al., 1996). Physiological parameters describing these GI compartments have been previously reported (Sjögren et al., 2013). The GI model is linked to a simulated systemic pharmacokinetic model, with up to three compartments, to enable simulations and predictions of the plasma concentration–time profiles. In GI-Sim drug particles and monomers flow from one GI compartment into the next. The particles either dissolve or grow, and the monomers partition into colloidal structures or are absorbed across the intestinal wall. The pH-dependent solubility of an ionizable compound in the lumen is calculated in GI-Sim according to the Henderson–Hasselbalch equation and the physiological pH of each GI compartment (Hasselbalch, 1916). The dissolution rate in GI-Sim is usually described by Fick's law and the Nielsen stirring model (Nielsen, 1961); however, in this study, the *in vitro* experimental release profiles of the formulations were used for the appearance rate of free monomer in the GI compartments. The effective intestinal permeability for each API was used to describe the total serial transport process across the aqueous boundary layer adjacent to the intestinal wall and the small intestine membrane (Lennernäs et al., 1996; Sandberg et al., 1991; Sjögren et al., 2013; Tubic-Grozdanis et al., 2008). Absorption occurs in all intestinal compartments including the colon (there is no absorption in the stomach). The relevant physicochemical, biopharmaceutical, and pharmacokinetic properties of the investigated APIs and formulations are summarized in Table 2. The AAFE was used to analyze

Table 2
Pharmacokinetic parameters used in *in vivo* simulations.

API	CL (l/h)	Vc (l)	k12 (h^{-1})	k21 (h^{-1})	First pass extraction (%)	P_{eff} (10^{-4} cm/s)
Metoprolol	54[a]	84[a]	6.7[a]	2.4[a]	30[a]	1.3[f]
Diclofenac	16[b]	3.1[b]	4.4[b]	41[b]	60[c]	3.1[g]
Naproxen	21[d]	4.0[d]	0.093[d]	0.14[d]	0[e]	8.5[f]
Carbamazepine	1.1[f]	60.7[f]	0.036[f]	0.24[f]	1.25[f]	4.3[f]

API: active pharmaceutical ingredient; CL: clearance; First pass: first pass metabolism; k12 and k21: distribution rate constants; P_{eff}: human effective jejunal permeability; V_c: volume of distribution.

[a] Sandberg et al. (1991).
[b] Rani et al. (2004).
[c] Peris-Ribera et al., (1991).
[d] Runkel et al. (1973).
[e] Yu and Amidon (1999).
[f] Sjögren et al. (2013).
[g] Tubic-Grozdanis et al. (2008).

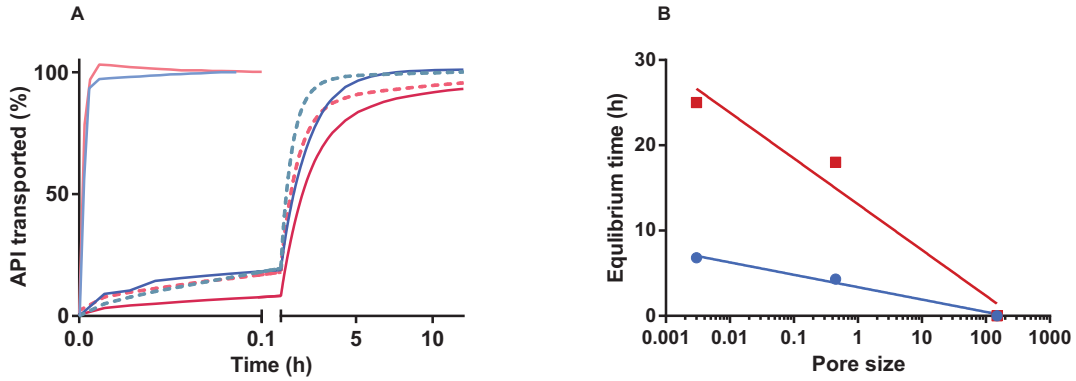

Fig. 2. (A) Transport of metoprolol and diclofenac in aqueous solution across three diffusion barriers. Metoprolol across the nylon mesh filter, 150 μm pores, (——); the polyvinylidene fluoride filter, 0.45 μm pores, (– – –); and the cellulose-based dialysis membrane, approximate pore size 0.003 μm, (——). Diclofenac across the nylon mesh filter (——); the polyvinylidene fluoride filter (– – –), and the cellulose-based dialysis membrane (——). All experiments were carried out at 37 °C with a stirring rate of 400 rpm. (B) Correlation between equilibrium time (h) and pore size described with a nonlinear semi-log function for diclofenac and metoprolol, $y = 3.4 - 1.5 * \log x, R^2 = 0.98$, and $y = 13 - 5.4 * \log x, R^2 = 0.96$, respectively. Metoprolol observed values (■) and the non-linear semi-log function values (——); diclofenac observed values (●) and the non-linear semi-log function values (——).

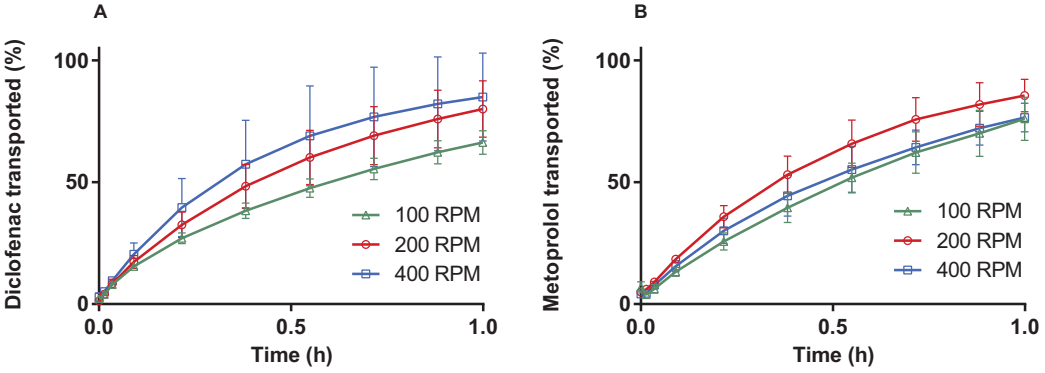

Fig. 3. (A) Effect of stirring rate on the transport of diclofenac in aqueous solution across the diffusion barrier. (B) Effect of stirring rate on the transport of metoprolol in aqueous solution across the diffusion barrier. Both experiments were performed at 37 °C with a polyvinylidene fluoride filter (0.45 μm pores) as diffusion barrier.

the goodness of fit between the predicted and observed plasma concentrations (Graham et al., 2012).

3. Results

3.1. Effect of diffusion barrier in the miniaturized release method

There was a correlation between the pore size of the diffusion barrier and the time to reach equilibrium (time to reach plateau) in the sample reservoir and the release medium (Fig. 2). The equilibrium times for diclofenac across the nylon mesh filter, the polyvinylidene fluoride filter and cellulose-based dialysis membrane were 0.011 h, 4.3 h and 6.8 h, respectively. For metoprolol, the equilibrium times were 0.011 h, 18 h and 25 h, respectively. The correlation between equilibrium time, y (h), and pore size, x (μm) was described as $y = 3.4 - 1.5 \times \log x$, $R^2 = 0.98$, and $y = 13 - 5.4 \times \log x$, $R^2 = 0.96$, for diclofenac and metoprolol, respectively. The time to equilibrium for the nylon mesh filter (with a pore size of 150 μm) was thus more than a hundred times shorter than that for the other two diffusion barriers: the polyvinylidene fluoride filter (with a pore size of 0.45 μm) and the cellulose-based dialysis membrane (with a pore size of 0.003 μm).

The influence of stirring rate on the API mass transport as a mean value of three observations, with the polyvinylidene fluoride filter as diffusion barrier, is shown in Fig. 3. The mass transport of diclofenac across the diffusion barrier was increasing with higher stirring rate. However, there was no correlation between the stirring rate and the mass transport of metoprolol. After 1 h of stirring at 100, 200 or 400 rpm, the mass transport of metoprolol across the diffusion barrier was 76%, 86%, and 77%, respectively.

Table 3
Interpretations of estimated exponent b values in the Weibull function according to Papadopoulou et al. (2006).

	Indicated release mechanism
$b < 0.39$	Not found in simulations. May occur in highly disordered spaces that are very different from percolation clusters.
$0.39 < b < 0.69$	Diffusion in fractal or disordered substrates, different from that in percolation clusters.
$b \approx 0.69 - 0.75$	Diffusion in normal Euclidian space.
$0.75 < b < 1$	Diffusion in normal Euclidian substrate with contribution from another release mechanism.
$b = 1$	First-order release.
$b > 1$	Sigmoid curve indicative of a complex release mechanism.

3.2. Indicated mechanisms of drug release

Interpretations of the b values in the Weibull function are summarized in Table 3 (Papadopoulou et al., 2006). The drug release profiles for each of the investigated DDSs are shown in Fig. 4 and the corresponding a and b estimates are listed in Table 4.

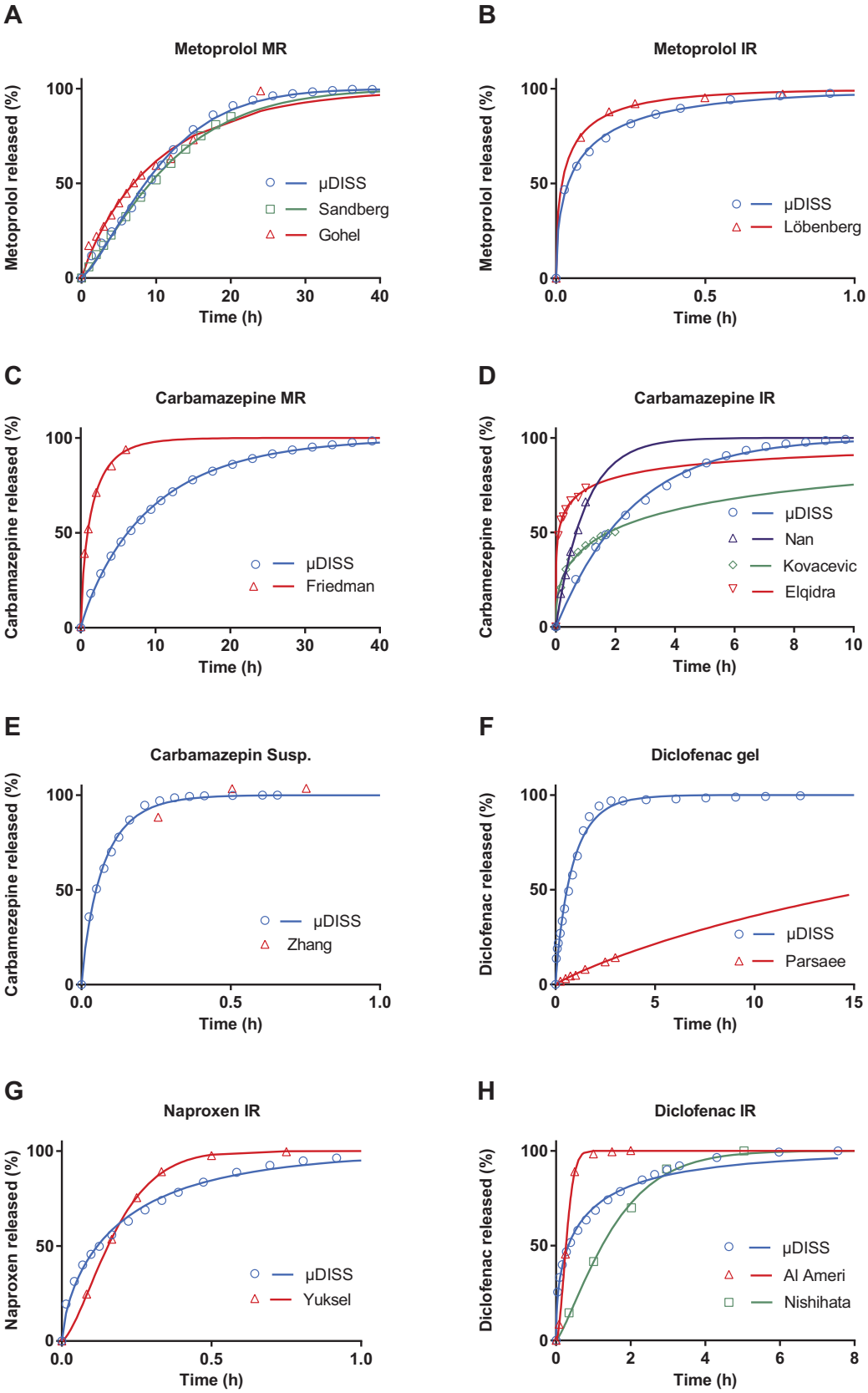

Fig. 4. *In vitro* drug release using data acquired with the novel, miniaturized, µDISS™ *in vitro* release method and historical *in vitro* data. Symbols represent the observed data and lines represent WinNonlin curve fitting of the Weibull function. (A) Release profile for metoprolol from a slurry of modified-release (MR) pellets using data from the miniaturized method and historical data (Gohel et al., 2009; Sandberg et al., 1988). (B) Release profile for metoprolol from a slurry of immediate-release (IR) metoprolol using miniaturized-method data and historical data (Löbenberg et al., 2005). (C) Release profile for carbamazepine from a slurry of MR carbamazepine using miniaturized-method data and historical data (Friedman et al., 2000). (D) Release profile for carbamazepine from a slurry of IR carbamazepine using miniaturized-method data and historical data (Elqidra et al., 2004; Kovacevic et al., 2008; Nan et al., 2012). (E) Release profile for carbamazepine from a carbamazepine oral suspension using miniaturized-method data and

Table 4
Estimation (CV%) of the Weibull function, using data obtained from the miniaturized experimental method (μDISS™) or historical data.

API	DDS	a	b	AAFE	Method	Medium	Reference
Naproxen IR	IR	3 (2.8)	0.69 (2.4)	1.06	Miniaturized	PBS pH 7.4	
		11 (2.9)	1.5 (1.2)	1.02	USP II	PBS pH 7.4	Yuksel et al. (2000)
Metoprolol	IR	3.5 (2.6)	0.5 (2.4)	1.02	Miniaturized	PBS pH 7.4	
		4.6 (6.5)	0.48 (6.7)	1.01	USP II	SGF	Löbenberg et al. (2005)
Diclofenac	IR	1.2 (1.2)	0.49 (2)	1.11	Miniaturized	PBS pH 7.4	
		7.7 (5.9)	1.8 (2.6)	1.03	USP II	0.1 N HCl	Al Ameri et al. (2012)
		0.53 (6.1)	1.3 (6.5)	1.04	Shaken beaker	PBS pH 6.8	Nishihata (1987)
Carbamazepine	IR	0.39 (1.8)	1 (1.4)	1.00	Miniaturized	PBS pH 7.4	
		1.3 (1.7)	0.27 (4.9)	1.01	USP II	1% SLS	Elqidra et al. (2004)
		1 (4.1)	1 (6.2)	1.06	Basket	0.1 mol/L HCl	Nan et al. (2012)
		0.55 (1.4)	0.4 (5.3)	1.04	USP II	PBS pH 6.8	Kovacevic et al. (2008)
Carbamazepine	MR	0.13 (1.3)	0.9 (0.6)	1.02	Miniaturized	PBS pH 7.4	
		0.74 (5)	0.72 (7.3)	1.95	USP II	1% SLS	Friedman et al. (2000)
Metoprolol	MR	0.039 (4.4)	1.3 (1.3)	1.06	Miniaturized	PBS pH 7.4	
		0.12 (14)	0.91 (7.4)	1.07	USP II	PBS pH 6.8	Gohel et al. (2009)
		0.046 (7.5)	1.2 (2.5)	1.07	USP II	PBS pH 6.8	Sandberg et al. (1988)
Carbamazepine	Susp	9.6 (6.1)	0.87 (2.8)	1.03	Miniaturized	PBS pH 7.4	
		NA*	NA*	NA*	USP II	Water	Zhang et al. (2011)
Diclofenac	Gel	1.1 (2.1)	0.89 (2.9)	1.15	Miniaturized	PBS pH 7.4	
		0.056 (3.6)	0.9 (4.4)	1.05	Franz cell	PBS pH 7.4	Parsaee et al. (2002)

AAFE: absolute average fold error; a and b: constants in the Weibull function estimated with WinNonlin; API: active pharmaceutical ingredient; CV: coefficient of variation; DDS: drug delivery system; Gel: dermal gel; IR: immediate-release tablet; MR: modified-release tablet; NA*: not available because of too few data points; PBS: phosphate buffered saline; SGF: simulated gastric fluid without enzymes; SLS: sodium lauryl sulfate; Susp: oral suspension; USP: United States Pharmacopeia.

The indicated types of drug release varied according to the methodology used. Drug release through a highly disordered space was indicated for one data set (IR carbamazepine) (Elqidra et al., 2004). Drug release governed by diffusion in a fractal or disordered substrate was indicated only by data for IR formulations, including both the miniaturized-method experimental data for IR naproxen, IR diclofenac and IR metoprolol and historical data for IR carbamazepine and IR metoprolol (Kovacevic et al., 2008; Löbenberg et al., 2005). Diffusion through a normal Euclidian space was the most plausible drug release mechanism for one historical set of MR carbamazepine data (Friedman et al., 2000). Diffusion through a normal Euclidian space with the contribution of another release mechanism was suggested by historical data for MR metoprolol (Gohel et al., 2009) and diclofenac gel (Gohel et al., 2009; Parsaee et al., 2002), and by the miniaturized-method experimental results for MR carbamazepine, the oral carbamazepine suspension, and diclofenac gel. A first-order release rate was indicated by both historical data (Nan et al., 2012) and the experimental results for IR carbamazepine. A sigmoidal release curve, interpreted as indicating a complex release mechanism, was suggested by historical data sets for IR naproxen (Yuksel et al., 2000), IR diclofenac (two data sets) (Al Ameri et al., 2012; Nishihata, 1987) and MR metoprolol Sandberg et al. (1988), as well as by experimental data for MR metoprolol. The historical data for the oral carbamazepine suspension had too few reported data points (first data point at 80% released) to be analyzed in this manner.

3.3. In silico simulations of in vivo response

The simulations of the plasma profiles obtained with GI-Sim were based on the miniaturized-method (μDISS™) or historical *in vitro* release profiles (Al Ameri et al., 2012; Elqidra et al., 2004; Friedman et al., 2000; Gohel et al., 2009; Kovacevic et al., 2008; Löbenberg et al., 2005; Nan et al., 2012; Nishihata, 1987; Parsaee et al., 2002; Reiner et al., 2001; Sandberg et al., 1988; Yuksel et al., 2000; Zhang et al., 2011; Zhou et al., 1998). The plasma-time concentration profiles and the AUCs, maximum concentrations (C_{max}) and times to C_{max} (t_{max}) from the experimental and simulated data are shown in Fig. 5 and Table 5, respectively. The agreement between the predicted concentration-time plasma profiles and the observations was assessed using the AAFE with the respective values at the times of the observations. In addition, the predictive ability was evaluated from the agreement between the observed and simulated PK parameters (AUC, t_{max} and C_{max}). In general, the simulations based on the data from the miniaturized *in vitro* method were in good agreement with the observed plasma profiles, with AAFE values in the range of 1.03–1.53. For five of the seven investigated DDSs (71%), the *in vivo* predictions (*i.e.*, the accuracy of AUC, t_{max} and C_{max} predictions) based on the miniaturized-method experimental data were equally or more accurate than the predictions based on historical *in vitro* release data. For the remaining two DDSs, MR metoprolol and IR carbamazepine, the *in vivo* prediction based on the miniaturized-method experimental data was less accurate than that based on two of the historical release data, with AAFE values of 1.53 and 1.31, respectively.

4. Discussion

Eight DDSs were investigated using a novel, miniaturized, *in vitro* drug-release method and *in silico* modeling. The benefits of this method include the ability to collect data continuously, the use of only small amounts of sample and release medium, and the

historical data (Zhang et al., 2011) (too few data points to perform curve fitting). (F) Release profile for diclofenac from diclofenac gel using miniaturized-method data and historical data (Parsaee et al., 2002). (G) Release profile for naproxen from a slurry of IR naproxen using miniaturized-method data and historical data (Yuksel et al., 2000). (H) Release profile for diclofenac from a slurry of IR diclofenac using miniaturized-method data and historical data (Al Ameri et al., 2012; Nishihata, 1987). *In vitro* drug release was measured with a 150 μm nylon mesh filter as diffusion barrier and 10 ml of PBS buffer, at a temperature of 37 °C, with a stirring rate of 400 rpm.

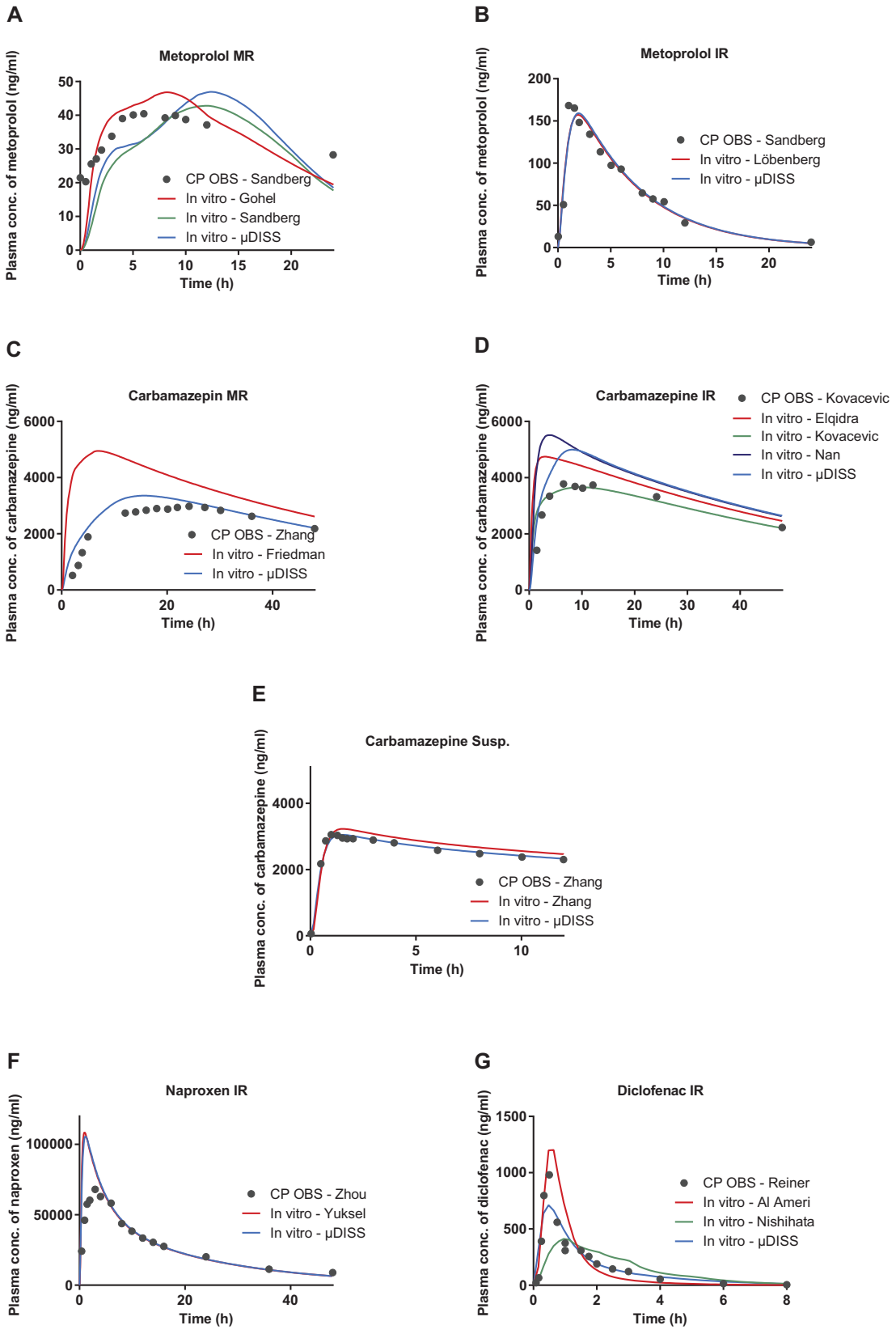

Fig. 5. Historical *in vivo* drug concentrations in plasma over time (CP OBS) and simulated (GI-Sim) *in vivo* plasma concentration-time profiles based on *in vitro* data obtained from the miniaturized method (µDISS™) (data acquired with a nylon mesh, pore size 150 µm) and historical sources. Symbols represent historical CP OBS, lines represent simulated plasma concentrations. (A) observed data from Sandberg et al. (1988), simulated red line data from Gohel et al. (2009), simulated green line data from Sandberg et al. (1988), and simulated blue line data from the miniaturized method. (B) observed data from Sandberg et al. (1988), red line data from Löbenberg et al. (2005) and blue line data from the miniaturized method. (C) observed data from Zhang et al. (2011), red line data from Friedman et al. (2000), and blue line data from the miniaturized method. (D)

Table 5
Pharmacokinetic parameters (AUC, C_{max}, t_{max}) from clinical observations (in **bold**) and *in vitro*-based *in silico* simulations (in *italics*).

API	DDS	AUC (ng*h/ml)	t_{max} (h)	C_{max} (ng/ml)	AAFE	Reference
Naproxen	IR	**1200000**	**3**	**68000**		Zhou et al. (1998)
		1300000	*1.1*	*110000*	1.26	Miniaturized method
		1300000	*0.96*	*110000*	1.27	Yuksel et al. (2000)
Metoprolol	IR	**1300**	**1**	**170**		Sandberg et al. (1988)
		1300	*1.9*	*160*	1.11	Miniaturized method
		1200	*1.9*	*160*	1.12	Löbenberg et al. (2005)
Diclofenac	IR	**1100**	**0.5**	**980**		Reiner et al. (2001)
		1200	*0.48*	*710*	1.42	Miniaturized method
		1200	*0.64*	*1200*	1.73	Al Ameri et al. (2012)
		1200	*0.96*	*410*	1.83	Nishihata (1987)
Carbamazepine	IR	**150000**	**6.5**	**3800**		Kovacevic et al. (2008)
		180000	*8.2*	*5000*	1.31	Miniaturized method
		170000	*1.9*	*4700*	1.39	Elqidra et al. (2004)
		190000	*4*	*5500*	1.52	Nan et al. (2012))
		140000	*9.6*	*3700*	1.12	Kovacevic et al. (2008)
Carbamazepine	MR	**120000**	**24**	**3000**		Zhang et al. (2011)
		130000	*16*	*3400*	1.24	Miniaturized method
		180000	*6.9*	*4900*	1.87	Friedman et al. (2000)
Metoprolol	MR	**820**	**6**	**40**		Sandberg et al. (1988)
		800	*12*	*47*	1.53	Miniaturized method
		820	*8.2*	*47*	1.30	Gohel et al. (2009)
		750	*12*	*43*	1.70	Sandberg et al. (1988)
Carbamazepine	Susp	**31000**	**0.99**	**3100**		Zhang et al. (2011)
		31000	*1.4*	*3100*	1.03	Miniaturized method
		33000	*1.6*	*3200*	1.08	Zhang et al. (2011)

AAFE: absolute average fold error; API: active pharmaceutical ingredient; AUC: area under the concentration-time curve; C_{max}: maximum concentration; DDS: drug delivery system; IR: immediate-release tablet; MR: modified-release tablet; Susp: oral suspension; t_{max}: time to C_{max}.

possibility of modifying the method by changing the diffusion barrier. The *in vitro* release profiles obtained using the miniaturized μDISS™ system were suitable for release mechanism analysis, and the predictability of *in vivo* behavior from the miniaturized-method data, evaluated using the biopharmaceutical *in silico* model GI-Sim (Sjögren et al., 2013) was generally more accurate than that from the historical data.

4.1. Evaluation of the diffusion barrier

The diffusion barrier investigation showed that the nylon mesh filter with 150 μm pores had only a minor impact on the equilibrium time (0.011 h), while the filters with smaller pores significantly increased the equilibrium time. There are several possible explanations for this observation. The pore size in the nylon mesh filter was presumably sufficiently large to facilitate the flow of fluids. Since the smaller pores reduced this fast fluid flow, the dominating mass transport mechanism across the dialysis membrane and the polyvinylidene filter may thus have been the slower molecular diffusion (Kostewicz et al., 2014b). The total available pore area determines the rate of mass transport when molecular diffusion is the main mechanism of transport. The two selected APIs, diclofenac and metoprolol, showed slightly different equilibrium times for the dialysis membrane which might be explained by different API affinity to the same dialysis membrane. Possibly, the positively charged metoprolol ($pK_a = 9.7$) is attracted to the negatively charged cellulose membrane while the negatively charged diclofenac is not ($pK_a = 3.8$). In all, care should be taken when choosing an appropriate diffusion barrier since the material may affect the equilibrium time. However, for DDSs such as emulsions, a dialysis membrane could prevent the formulation from spreading outside the sample reservoir, thereby reducing the pharmaceutical effect of the excipients on the UV measurements as well as better control of the available total surface area for release (Morais and Burgess, 2014). If the diffusion barrier influences the API mass transport, this effect needs to be evaluated and corrected for in future data analyses (Levy and Benita, 1990; Washington, 1989).

A stirring rate of 400 rpm allowed sufficiently fast mass transport across the nylon mesh to minimize any influence on the drug-release profiles. However, further hydrodynamic investigation of the influence of the stirring rate on mass transport in the miniaturized release method is needed and is currently on-going.

4.2. Interpretation of the in vitro drug-release mechanism from drug delivery systems

The use of the Weibull function, suggested by Papadopoulou et al. (2006) facilitates straightforward analysis of drug-release mechanisms and is applicable for a wide range of formulations and types of mechanism. The release of the drug in fractal or disordered matrices appears to be driven only by diffusion. Diffusion in irregular fractal spaces is slower than in a homogeneous Euclidian space (Kosmidis et al., 2003a). Diffusion in a homogeneous space

observed data from Kovacevic et al. (2008), red line data from Elqidra et al. (2004), green line data from Kovacevic et al. (2008), purple line data from Nan et al. (2012), and blue line data from the miniaturized method. (E) observed data from Zhang et al. (2011), red line data from Zhang et al. (2011), and blue line data from the miniaturized method. (F) observed data from Zhou et al. (1998), red line data from Yuksel et al. (2000), and blue line data from the miniaturized method. (G) observed data from Reiner et al. (2001), red line data from Al Ameri et al. (2012), green line data from Nishihata et al. (1987), and blue line data from the miniaturized method. (For interpretation of the references to colour in this figure legend, the reader is referred to the web version of this article.)

when another release mechanism also is involved indicates diffusion-driven release with additional input from case II transport. In case II transport, the relaxation of the tablet matrix polymers influences the movement of the APIs through the matrix (Kosmidis et al., 2003c). First-order drug release follows Fick's law of diffusion (Papadopoulou et al., 2006). A sigmoidal release curve is indicative of a complex release mechanism, involving erosion-based release or the release of a relatively insoluble API (Kosmidis et al., 2003b; Papadopoulou et al., 2006).

The drug-release mechanisms for seven of the IR formulation data sets (see Table 4) were, in accordance with theory and formulation strategy, based on diffusion through a fractal/disordered matrix or diffusion according to Fick's law (first-order release). In contrast, the data sets for IR naproxen and IR diclofenac suggested complex release mechanisms involving erosion or influence of the relative insolubility of the APIs (Kosmidis et al., 2003b).

The release kinetics for the individually coated pellets of MR metoprolol indicated almost zero-order release over 24 h (Sandberg et al., 1988). To provide a drug release mechanism that follows zero-order kinetics, the DDS must be designed to overcome Fick's law of diffusion, in which the diffusion is non-linear over time due to the changes in surface area and diffusion length (Chidambaram et al., 1998). Therefore, a more complex mechanism is required; this can be achieved, for example, by coating the pellets, as seen with the ethylcellulose coating used in MR metoprolol (Sandberg et al., 1988; Varelas et al., 1995). For the three MR metoprolol data sets, the indicated release mechanisms were either a complex mechanism or diffusion-controlled in combination with case II transport. Hence, the indicated release mechanisms for MR metoprolol are in line with the reported approximate zero-order release (Sandberg et al., 1988).

For MR carbamazepine, the release mechanism indicated by the miniaturized-method data was different from that indicated by the historical data (see Table 4) (Friedman et al., 2000). API release was driven only by diffusion in the historical data set, while the miniaturized-method data set indicated the presence of diffusion with contribution from case II transport. When MR carbamazepine is used clinically, the patient is instructed not to crush the tablets. However, the prolonged *in vitro* release from the crushed tablet indicated that the individually coated pellets of the MR tablet remained intact (Kesarwani et al., 2007).

The difference in the rate of drug release from diclofenac gel between data obtained using the miniaturized method and historical data was probably due to the large difference in pore size (more than a 50,000-fold difference) between the diffusion barriers. Nylon mesh (150 μm pores) was used in the miniaturized method, whereas a cellulose acetate dialysis membrane with a molecular weight cut-off point of 1000 was used for collection of the historical data (Parsaee et al., 2002).

In the novel, miniaturized, μDISS^{TM} *in vitro* method, only a representative proportion of each DDS was investigated whereas, in the historical release methods, an intact formulation unit such as a tablet was examined. While the surface area of the diffusion barrier was constant during the miniaturized-method experiments, the surface area of the particles was not constant. The historical *in vitro* release experiments differed in the applied release equipment and set-ups, such as stirring rate, release medium (*e.g.*, differing in pH and/or the addition of surfactant), as well as in the volume of release medium used (Al Ameri et al., 2012; Elqidra et al., 2004; Friedman et al., 2000; Gohel et al., 2009; Kovacevic et al., 2008; Löbenberg et al., 2005; Nan et al., 2012; Nishihata, 1987; Parsaee et al., 2002; Sandberg et al., 1988; Yuksel et al., 2000; Zhang et al., 2011). Therefore, the *in vitro* release profile and consequently the indicated release mechanism varied for the investigated DDS. As an example, the four *in vitro* data sets for IR carbamazepine differed with regard to the release method and the release medium used, and consequently the *b* values ranged between 0.27 and 1.0. The DDS for IR metoprolol was the exception; the same release mechanism was indicated in both the miniaturized-method and historical data sets. As expected, the release mechanism differed between the IR, MR and non-solid drug delivery systems. In conclusion, there was wide variation in the indicated release mechanisms between the data sets. The differences in method set-ups seemed to affect the drug release to a greater extent than the differences caused by using a representative part of the DDS or an intact unit.

4.3. Gastrointestinal (GI) absorption simulation

In vitro data originating from both the miniaturized method and the historical investigations for four model drugs were inserted into the *in silico* model GI-Sim to predict the plasma concentration-time profiles *in vivo*. The *in vitro* release profiles as well as selected parameters listed in Tables 1 and 2 determined the predicted *in vivo* response. As shown in Fig. 4 the *in vitro* release method had an impact on the release profiles and consequently on the predicted plasma-time profiles. Based on the *in vitro* drug-release profiles, GI drug absorption was predicted to occur mainly from the proximal small intestine or throughout the whole intestine including the colon. The potential for colonic absorption will be relevant for DDSs with prolonged drug-release profiles (>3 h), such as MR metoprolol, MR carbamazepine, and IR carbamazepine, as the specified mean transit time to reach the colon in GI-Sim is 3.5 h (Sjögren et al., 2013). Overall, the experimental data acquired with the novel, miniaturized, *in vitro* μDISS^{TM} method gave more accurate predictions of the plasma concentration profiles than the historical *in vitro* data. The predictions based on the miniaturized method data were equally or more accurate than the predictions based on historical *in vitro* release data for 71% of the investigated DDSs. This was the case for both IR and MR formulations, indicating the overall accuracy of the modified miniaturized method. However, for IR carbamazepine and MR metoprolol one historical *in vitro* release data set for each formulation gave more accurate predictions. The *in vivo* profile for MR carbamazepine was very well described by the *in vitro* data, while the *in vitro* data for IR carbamazepine were somewhat less predictive. This appears contradictory, as it could be assumed that the *in vitro* drug-release profile for an IR formulation would be more likely to reflect the *in vivo* release profile. The inaccurate prediction for the IR formulation was also observed for two historical data sets (Elqidra et al., 2004; Nan et al., 2012). The *in vivo* predictions based on the *in vitro* data set from Kovacevic et al. were, however, accurate (Kovacevic et al., 2008). It is noteworthy that, in this investigation of the IR formulation, only 50% of the carbamazepine was released in 2 h (Kovacevic et al., 2008). The administered dose was predicted to be incompletely absorbed throughout the small and large intestine as a consequence of this slow release. For MR metoprolol, the *in vitro* release of the three data sets are quite similar (see Fig. 4), however, the predicted plasma-time profiles (see Fig. 5) are not. One *in vitro* release data set (Gohel et al., 2009) have a slightly higher drug release compared to the miniaturized method which lead to a higher absorption of metoprolol before the colon compartment of GI-Sim. This might be explained by a delay in the predicted t_{max} when based on release data from the miniaturized method.

In this study, the combination of *in vitro* and *in silico* tools was a valuable asset for the evaluation of the *in vivo* predictive performance of the *in vitro* results. This advantageous combination has been shown previously, and there is an ongoing effort to further improve these synergistic methodologies (Kostewicz et al., 2014a; Lennernäs et al., 2014b).

5. Conclusion

The developed *in vitro* release method based on the miniaturized μDISS™ technique enables continuous sampling with small volumes of both DDS (21 μl) and release medium (10 ml). In this experimental study, *in vitro* release data were collected from eight selected DDSs with four APIs. Collection of API release data was possible for both solid and non-solid formulations, as well as for charged and uncharged APIs. Both the miniaturized-method and the historical release data were used to estimate the release mechanisms and to predict the plasma concentration-time profiles in a biopharmaceutical GI absorption model (Al Ameri et al., 2012; Elqidra et al., 2004; Friedman et al., 2000; Gohel et al., 2009; Kovacevic et al., 2008; Löbenberg et al., 2005; Nan et al., 2012; Nishihata, 1987; Parsaee et al., 2002; Reiner et al., 2001; Sandberg et al., 1988; Sjögren et al., 2013; Yuksel et al., 2000; Zhang et al., 2011; Zhou et al., 1998). The indicated release mechanisms for the APIs varied according to the source of the data. This discrepancy most likely originated from differences in the methods used, such as the stirring rate, the release medium used, and the *in vitro* apparatus used. For five of the seven evaluable drug formulations, predictions of the *in vivo* plasma concentration-time profiles obtained using the novel, miniaturized, μDISS™ *in vitro* data were at least as accurate as those obtained from the historical *in vitro* data. These promising results could reduce the amounts of the formulations and release media required in the collection of *in vitro* data, while still generating accurate *in vivo* predictions.

Acknowledgements

Financial support was provided by the Swedish Research Council, grant number 521-2011-373. Laboratory assistance from Marcus Wanselius was greatly valued. This work was contributed to the EU IMI project OrBiTo (www.orbitoproject.eu) as side ground.

References

Al Ameri, M.N., Nayuni, N., Anil Kumar, K.G., Perrett, D., Tucker, A., Johnston, A., 2012. The differences between the branded and generic medicines using solid dosage forms: in-vitro dissolution testing. Results Pharm. Sci. 2, 1–8.
Avdeef, A., Tsinman, K., Tsinman, O., Sun, N., Voloboy, D., 2009. Miniaturization of powder dissolution measurement and estimation of particle size. Chem. Biodivers. 6, 1796–1811.
Avdeef, A., Tsinman, O., 2008. Miniaturized rotating disk intrinsic dissolution rate measurement: effects of buffer capacity in comparisons to traditional Wood's apparatus. Pharm. Res. 25, 2613–2627.
Benet, L.Z., Broccatelli, F., Oprea, T.I., 2011. BDDCS applied to over 900 drugs. AAPS J. 13, 519–547.
Bijlani, V., Yuonayel, D., Katpally, S., Chukwumezie, B.N., Adeyeye, M.C., 2007. Monitoring ibuprofen release from multiparticulates: in situ fiber-optic technique versus the HPLC method: a technical note. AAPS PharmSciTech 8, E9–E12.
Chidambaram, N., Porter, W., Flood, K., Qiu, Y., 1998. Formulation and characterization of new layered diffusional matrices for zero-order sustained release. J. Control. Release 52, 149–158.
Dash, S., Murthy, P.N., Nath, L., Chowdhury, P., 2010. Kinetic modeling on drug release from controlled drug delivery systems. Acta Pol. Pharm. 67, 217–223.
Elqidra, R., Unlu, N., Çapan, Y., Sahin, G., Dalkara, T., Hincal, A., 2004. Effect of polymorphism on in vitro-in vivo properties of carbamazepine conventional tablets. J. Drug Deliv. Sci. Technol. 14, 147–153.
Fagerberg, J.H., Tsinman, O., Sun, N., Tsinman, K., Avdeef, A., Bergström, C.A., 2010. Dissolution rate and apparent solubility of poorly soluble drugs in biorelevant dissolution media. Mol. Pharm. 7, 1419–1430.
Fagerholm, U., Lindahl, A., Lennernäs, H., 1997. Regional intestinal permeability in rats of compounds with different physicochemical properties and transport mechanisms. J. Pharm. Pharmacol. 49, 687–690.
Friedman M., Golander Y., Kaplan R., Levitt B., Licht D., Moros D., Yacobi A., Zholkovsky M., 2000. Sustained release carbamazepine formulation, Google Patents.
Gohel, M.C., Parikh, R.K., Nagori, S.A., Jena, D.G., 2009. Fabrication of modified release tablet formulation of metoprolol succinate using hydroxypropyl methylcellulose and xanthan gum. AAPS PharmsciTech 10, 62–68.
Graham, H., Walker, M., Jones, O., Yates, J., Galetin, A., Aarons, L., 2012. Comparison of in-vivo and in-silico methods used for prediction of tissue: plasma partition coefficients in rat. J. Pharm. Pharmacol. 64, 383–396.
Hasselbalch, K., 1916. The calculation of the hydrogen number of the blood from the free and bound carbon dioxide of the same and the binding of oxygen by the blood as a function of the hydrogen number. Biochem. Z. 78, 112–144.
Johannsson, G., Nilsson, A., Bergthorsdottir, R., Burman, P., Dahlqvist, P., Ekman, B., Engström, B., Olsson, T., Ragnarsson, O., Ryberg, M., 2011. Improved cortisol exposure-time profile and outcome in patients with adrenal insufficiency: a prospective randomized trial of a novel hydrocortisone dual-release formulation. J. Clini. Endocrinol. Metab. 97, 473–481.
Kesarwani A., Chawla M., Raghuvanshi R., Rampal A., 2007. Multiple unit modified release compositions of carbamazepine and process for their preparation, Google Patents.
Klein, S., 2010. The use of biorelevant dissolution media to forecast the in vivo performance of a drug. AAPS J. 12, 397–406.
Kosmidis, K., Argyrakis, P., Macheras, P., 2003a. Fractal kinetics in drug release from finite fractal matrices. J. Chem. Phys. 119, 6373–6377.
Kosmidis, K., Argyrakis, P., Macheras, P., 2003b. A reappraisal of drug release laws using Monte Carlo simulations: the prevalence of the weibull function. Pharm. Res. 20, 988–995.
Kosmidis, K., Rinaki, E., Argyrakis, P., Macheras, P., 2003c. Analysis of Case II drug transport with radial and axial release from cylinders. Int. J. Pharm. 254, 183–188.
Kostewicz, E.S., Aarons, L., Bergstrand, M., Bolger, M.B., Galetin, A., Hatley, O., Jamei, M., Lloyd, R., Pepin, X., Rostami-Hodjegan, A., Sjögren, E., Tannergren, C., Turner, D.B., Wagner, C., Weitschies, W., Dressman, J., 2014a. PBPK models for the prediction of in vivo performance of oral dosage forms. Eur. J. Pharm. Sci. 57, 300–321.
Kostewicz, E.S., Abrahamsson, B., Brewster, M., Brouwers, J., Butler, J., Carlert, S., Dickinson, P.A., Dressman, J., Holm, R., Klein, S., Mann, J., McAllister, M., Minekus, M., Muenster, U., Müllertz, A., Verwei, M., Vertzoni, M., Weitschies, W., Augustijns, P., 2014b. In vitro models for the prediction of in vivo performance of oral dosage forms. Eur. J. Pharm. Sci. 57, 342–366.
Kovacevic, I., Parojcic, J., Homšek, I., Tubic-Grozdanis, M., Langguth, P., 2008. Justification of biowaiver for carbamazepine, a low soluble high permeable compound, in solid dosage forms based on IVIVC and gastrointestinal simulation. Mol. Pharm. 6, 40–47.
Larsen, S.W., Østergaard, J., Yaghmur, A., Jensen, H., Larsen, C., 2013. Use of in vitro release models in the design of sustained and localized drug delivery systems for subcutaneous and intra-articular administration. J. Drug Deliv. Sci. Technol. 23, 315–324.
Lennernäs, H., Aarons, L., Augustijns, P., Beato, S., Bolger, M., Box, K., Brewster, M., Butler, J., Dressman, J., Holm, R., 2014a. Oral biopharmaceutics tools–time for a new initiative–an introduction to the IMI project OrBiTo. Eur. J. Pharm. Sci. 57, 292–299.
Lennernäs, H., Abrahamsson, P., Langguth, B., 2014b. Oral biopharmaceutics-current status and identified gaps of understanding. Eur. J. Pharm. Sci. 57, 98.
Lennernäs, H., Palm, K., Fagerholm, U., Artursson, P., 1996. Comparison between active and passive drug transport in human intestinal epithelial (Caco-2) cells in vitro and human jejunum in vivo. Int. J. Pharm. 127, 103–107.
Levy, M.Y., Benita, S., 1990. Drug release from submicronized o/w emulsion: a new in vitro kinetic evaluation model. Int. J. Pharm. 66, 29–37.
Löbenberg, R., Kim, J.S., Amidon, G.L., 2005. Pharmacokinetics of an immediate release, a controlled release and a two pulse dosage form in dogs. Eur. J. Pharm. Biopharm. 60, 17–23.
Morais, J.M., Burgess, D.J., 2014. In vitro release testing methods for vitamin E nanoemulsions. Int. J. Pharm. 475, 393–400.
Nan, Z., Lijun, G., Tao, W., Dongqin, Q., 2012. Evaluation of carbamazepine (CBZ) supersaturatable self-microemulsifying (S-SMEDDS) formulation in-vitro and in-vivo. Iran. J. Pharm. Res. 11, 257.
Nielsen, A.E., 1961. Diffusion controlled growth of a moving sphere: the kinetics of crystal growth in potassium perchlorate precipitation. J. Phys. Chem. 65, 46–49.
Nishihata, T., 1987. Simple formulation of sustained-release tablets of sodium diclofenac and examination in humans. Int. J. Pharm. 40, 125–128.
O'Connor, K.M., Corrigan, O.I., 2001. Comparison of the physicochemical properties of the *N*-(2-hydroxyethyl) pyrrolidine, diethylamine and sodium salt forms of diclofenac. Int. J. Pharm. 222, 281–293.
Olsson, C.O.A., Landolt, D., 2003. Passive films on stainless steels—chemistry, structure and growth. Electrochim. Acta 48, 1093–1104.
Papadopoulou, V., Kosmidis, K., Vlachou, M., Macheras, P., 2006. On the use of the Weibull function for the discernment of drug release mechanisms. Int. J. Pharm. 309, 44–50.
Parsaee, S., Sarbolouki, M.N., Parnianpour, M., 2002. In-vitro release of diclofenac diethylammonium from lipid-based formulations. Int. J. Pharm. 241, 185–190.
Peris-Ribera, J.-E., Torres-Molina, F., Garcia-Carbonell, M.C., Aristorena, J.C., Pla-Delfina, J.M., 1991. Pharmacokinetics and bioavailability of diclofenac in the rat. J. Pharmacokinet. Biopharm. 19, 647–665.
Ragnarsson, G., Sandberg, A., Jonsson, U.E., Sjögren, J., 1987. Development of a new controlled release metoprolol product. Drug Dev. Ind. Pharm. 13, 1495–1509.
Rani, M., Surana, R., Sankar, C., Mishra, B., 2004. Formulation and biopharmaceutical evaluation of osmotic matrix tablets of diclofenac sodium. Drug Deliv. 11, 263–270.
Reiner, V., Reiner, A., Reiner, G., Conti, M., 2001. Increased absorption rate of diclofenac from fast acting formulations containing its potassium salt. Arzneimittelforschung 51, 885–890.

Runkel, R., Forchielli, E., Boost, G., Chaplin, M., Hill, R., Sevelius, H., Thompson, G., Segre, E., 1973. Naproxen-metabolism, excretion and comparative pharmacokinetics. Scand. J. Rheumatol. 2, 29–36.
Sandberg, A., Abrahamsson, B., Sjögren, J., 1991. Influence of dissolution rate on the extent and rate of bioavailability of metoprolol. Int. J. Pharm. 68, 167–177.
Sandberg, A., Blomqvist, I., Jonsson, U.E., Lundborg, P., 1988. Pharmacokinetic and pharmacodynamic properties of a new controlled-release formulation of metoprolol: a comparison with conventional tablets. Eur. J. Clin. Pharmacol. 33, S9–S14.
Scheytt, T., Mersmann, P., Lindstädt, R., Heberer, T., 2005. 1-Octanol/water partition coefficients of 5 pharmaceuticals from human medical care: carbamazepine, clofibric acid, diclofenac, ibuprofen, and propyphenazone. Water, Air, Soil Pollut. 165, 3–11.
Selen, A., Dickinson, P.A., Müllertz, A., Crison, J.R., Mistry, H.B., Cruañes, M.T., Martinez, M.N., Lennernäs, H., Wigal, T.L., Swinney, D.C., Polli, J.E., Serajuddin, A. T.M., Cook, J.A., Dressman, J.B., 2014. The biopharmaceutics risk assessment roadmap for optimizing clinical drug product performance. J. Pharm. Sci. 103, 3377–3397.
Shen, J., Burgess, D.J., 2012. Accelerated in-vitro release testing methods for extended-release parenteral dosage forms. J. Pharm. Pharmacol. 64, 986–996.
Siepmann, J., Siepmann, F., 2008. Mathematical modeling of drug delivery. Int. J. Pharm. 364, 328–343.
Siepmann, J., Siepmann, F., 2012. Modeling of diffusion controlled drug delivery. J. Control. Release 161, 351–362.
Sjögren, E., Tammela, T.L., Lennernäs, B., Taari, K., Isotalo, T., Malmsten, L.-Å., Axen, N., Lennernas, H., 2014. Pharmacokinetics of an injectable modified-release 2-hydroxyflutamide formulation in the human prostate gland using a semiphysiologically based biopharmaceutical model. Mol. Pharm. 11, 3097–3111.
Sjögren, E., Westergren, J., Grant, I., Hanisch, G., Lindfors, L., Lennernäs, H., Abrahamsson, B., Tannergren, C., 2013. In silico predictions of gastrointestinal drug absorption in pharmaceutical product development: Application of the mechanistic absorption model GI-Sim. Eur. J. Pharm. Sci. 49, 679–698.
Tsinman, K., Avdeef, A., Tsinman, O., Voloboy, D., 2009. Powder dissolution method for estimating rotating disk intrinsic dissolution rates of low solubility drugs. Pharm. Res. 26, 2093–2100.
Tubic-Grozdanis, M., Bolger, M.B., Langguth, P., 2008. Application of gastrointestinal simulation for extensions for biowaivers of highly permeable compounds. AAPS J. 10, 213–226.
Varelas, C.G., Dixon, D.G., Steiner, C.A., 1995. Zero-order release from biphasic polymer hydrogels. J. Control. Release 34, 185–192.
Washington, C., 1989. Evaluation of non-sink dialysis methods for the measurement of drug release from colloids – effects of drug partition. Int. J. Pharm. 56, 71–74.
Wu, C.-Y., Benet, L.Z., 2005. Predicting drug disposition via application of bcs: transport/absorption/elimination interplay and development of a biopharmaceutics drug disposition classification system. Pharm. Res. 22, 11–23.
Yu, L.X., Amidon, G.L., 1999. A compartmental absorption and transit model for estimating oral drug absorption. Int. J. Pharm. 186, 119–125.
Yu, L.X., Lipka, E., Crison, J.R., Amidon, G.L., 1996. Transport approaches to the biopharmaceutical design of oral drug delivery systems: prediction of intestinal absorption. Adv. Drug Deliv. Rev. 19, 359–376.
Yuksel, N., Kanık, A.E., Baykara, T., 2000. Comparison of in vitro dissolution profiles by ANOVA-based, model-dependent and -independent methods. Int. J. Pharm. 209, 57–67.
Zhang, X., Lionberger, R.A., Davit, B.M., Lawrence, X.Y., 2011. Utility of physiologically based absorption modeling in implementing quality by design in drug development. AAPS J. 13, 59–71.
Zhou, D., Zhang, Q., Lu, W., Xia, Q., Wei, S., 1998. Single- and multiple-dose pharmacokinetic comparison of a sustained-release tablet and conventional tablets of naproxen in healthy volunteers. J. Clin. Pharmacol. 38, 625–629.